International Journal of Thin Films Science and Technology

http://dx.doi.org/10.12785/ijtfst/030302

Magnetic Properties of Textured Nanocrystalline Mn-Zn Ferrite Thin Films Fabricated by Pulsed Laser Deposition.

Jaison Joseph[1,*] , *R. B. Tangsali*[2], *R.J.Choudhary*[3], *D. M. Phase*[3] *and V.Ganeshan*[3]

1Department of Physics, Govt. College, Khandola, Goa, India.

2Department of Physics, Goa University, Taleigao Plateau, Goa, India

3 UGC-DAE-CSR Indore 452 017

Email: jaisonjosephp@gmail.com

Received: 7 Jun. 2014, Revised: 21 Aug. 2014, Accepted: 23 Aug. 2014
Published online: 1 Sep. 2014

Abstract: $Mn_xZn_{1-x}Fe_2O_4$ nanoparticles were chemically synthesized by co- precipitating metal ions in alkaline aqueous solutions. The XRD peaks match up to spinel ferrites without any multi phase indication and clear visibility of ferrite FT-IR absorption bands confirm single phase spinal formation. Particle size derived from XRD data is authenticated by TEM micrographs. Thin films fabricated from this material on quartz substrate by pulse laser deposition were characterised using XRD. The XRD data revealed formation of spinel structure with a reasonable degree of texture. AFM analysis confirms nano granular film morphology with dimensions comparable to that of target grain. Magnetic data obtained from textured nanocrystalline Mn-Zn **f**errite thin film measurements made known enhanced coercivity. The observed enhanced coercivity is explained with due consideration of film texture and surface disorder that originated from Mn concentration specific initial adsorption prior to nucleation, resulting in directional film growth.

Keywords: Nanostructures, vacuum deposition, thin films, crystal structure, magnetic properties

1. Introduction

The variation in physical properties and its optimal utilization in emerging technologies made nanoparticle systems a subject of continuous interest. A combination of superb electrical and soft magnetic properties made spinal ferrites commercially significant. The co-existence of high relative magnetic and electric polarization along with high electrical resistivity makes these materials matchless in the present day electronic industry. Mixed spinel ferrites, essentially with low hysteresis loss and small particle sizes, have also found new applications in areas like targeted drug delivery systems and hyperthermia [1].

Ferrite thin films with spinel structure acquired scientific interest due to promising high-frequency applications, wherein low conductivity when compared to metal films is an important asset. The high saturation magnetization of ferrites compared to garnet-structure materials is also a preferable parameter of interest. This makes ferrite thin films a prime candidate for thin film high-frequency microwave device applications [2]. Large scale industrial applications require ferrite films to be grown in processes that are compatible with integrated circuit technology employing amorphous substrates. A low processing temperature is one preferred prerequisite requirement essential to block the possibility of unwanted chemical reactions with metal atoms in the device structures, during the integration of magnetic oxides with semiconducting materials. In pulse laser deposition process (PLD), high kinetic energy of target material in laser plume offers unique advantage of increased mobility for deposition of the material on the substrate in comparison to the other techniques. This results in creation of homogeneous film microstructure and helps in maintaining the stoichiometry of the target material. Further this technique preferably requires a lower substrate temperature also known as substrate processing temperature for crystallization of the thin film material.

Manganese zinc ferrite (Mn-Zn ferrite) finds applications in magnetic sensors, reading heads for magnetic recording media, switch mode power supplies, deflection yoke rings and spintronic devices in addition to large scale biomedical applications [1, 3-6]. Mn-Zn ferrite material in thin film form find process applications in

budding complex geometrical devices, such as magnetic recording heads for high density recording beyond Tb/inch^2, wherein a possible thermally assisted magnetic recording method can overcome the thermal agitation limit. [7] .To achieve this a magnetic recording field along with laser beam needs to be focused on to the same position over the recording media. However, incorporating a magnetic core in recording head which can generate sufficiently large field without any optical path interference to the laser beam is a design challenge. Mn-Zn ferrite thin films which are transparent magnetic materials with high *M*s and resistivity [8] could possibly be a potential candidate for use as magnetic core which can facilitate an uninterrupted optical path to the laser beam.

Hae Seok Cho investigated the effects of additives on the preferred orientations in Mn–Zn ferrite thin films deposited by ion beam sputtering on SiO_2 substrate at 350°C [9]. Y. Suzuki had grown epitaxial spinel ferrite thin films of Mn-Zn ferrite on $SrTiO_3$ and $MgAl_2O_4$ buffered by spinel structure [10]. Masaki Nakano used laser ablation technique contained with a shadow mask in Ar atmosphere to obtain crystalline Mn-Zn ferrite thin films on glass substrates at room temperature [11]. M. Koleva studied the magnetic behavior of Mn-Zn ferrite thin films deposited on silicon and sapphire substrates with and without a buffer layer of MgO [12]. Yan Liu produced $MnZnFe_2O_4$ thin films with various Zn content on Si substrate by alternately sputtering from two targets with the composition of $MnFe_2O_4$ and $ZnFe_2O_4$ respectively [13]. Hideki Etoh investigated the basic properties of Mn-Zn ferrite thin films fabricated by pulsed laser deposition with the aim of controlling their saturation magnetizations and electrical resistivity [14]. In all above referred studies the base material used for preparation of thin films is bulk in nature.

In our present study, the ferrite thin films were fabricated on quartz substrate from nano crystalline target material. The grown films with a reasonable degree of texture indicate nano granular morphology with dimensions comparable to that of target material. The observed enhancement in magnetic properties were explained with due consideration of surface roughfeness, originated from directional film growth. A nucleation process, which dependents on target chemical composition specific initial adsorption on to the substrate, may have resulted in directional film growth.

2. Experimental details

Nanoparticle $Mn_xZn_{1-x}Fe_2O_4$ ferrite material with (x= 0.4, 0.6 & 0.8) were prepared by co-precipitating aqueous solutions of $ZnSO_4$, $MnCl_2$ and $FeCl_3$ mixtures in alkaline medium. $ZnSO_4$:$7H_2O$, $MnCl_2$:$6H_2O$ and $FeCl_3$:$6H_2O$ were taken in respective stoichiometric proportions, dissolved in distilled water and heated up to 65^0C. The respective metal ions were precipitated by adding a suitable precipitating reagent, to the solution in boiling state under constant stirring within a time interval of 10 seconds. The mixture is then cooled down to a temperature of 80^0C. The mixture with the precipitate is maintained at 80^0C for one hour, prior to filtering of the precipitate. The precipitate was dried at 100^0C to remove the moisture and subjected to grinding in a pestal mortar. The powder was pelletized and sintered at a desired temperature for 15 hours, resulted in formation of $Mn_xZn_{1-x}Fe_2O_4$ nanoparticles.The powdered samples were characterized using Rigaku X-ray diffractometer with a high intensity rotating anode X-ray source. FT-IR absorption spectra of the samples were recorded on a Shimadzu 8900 FT-IR spectrometer. TEM micrographs were taken on a Hitachi-H-7650 machine.

The powder samples where palletised at 15 Ton pressure and sintered at 450^0C temperature to be used as target material for laser abletation. The laser ablations of the pallets were carried out at a chamber pressure of $2x10^{-6}$T on quartz substrate using Excimer laser KrF (248 nm) (Lambda Physik COMPex 201 model).The substrate temperature is maintained at 450^0C using an appropriate resistance heating system mounted on heater plate. The deposition was performed for 30 minutes with a target to substrate distance of 4.5cm, maintaining laser energy at 220 mJ. The pulse laser repetition rate was fixed at 10 Hz. The focused laser beam was incident on the target surface at an angle of 45°.The target was made to rotate with a rotation rate of 10 rpm. After deposition, the films were cooled to room temperature at the rate of 5 °C/min, maintaining vacuum chamber pressure. The fabricated thin films were characterized using Bruker AXE D8 X-ray Diffractometer with Cu Kα radiation at room temperature in standard θ/2θ mode. The thickness measurements of the films were carried out on AMBIOS XP-1 stylus profiler with 0.5 nm resolution. The surface morphologies of the films were investigated using AFM images taken on SPM (Digital Nano-Scope-III) in contact mode. Magnetic measurements were carried out on Quantum Design's MPMS SQUID VSM.

3. Results and Discussion

The X-ray diffraction (XRD) pattern of nanoparticle $Mn_xZn_{1-x}Fe_2O_4$ in powder form is as shown in Fig.1. The positions of observed peaks were in good agreement with reported values which confirm single phase cubic spinel structure of the samples. The interplanar spacing (d) was obtained from XRD data in accordance with Bragg's law and calculated the average lattice parameter 'a' using Eq.1. The grain size of the samples were estimated by executing Debye Scherrer equation (Eq.2) for all seven major spinnel peaks in each sample, followed by averaging of calculated grain size values with respect to each peak.

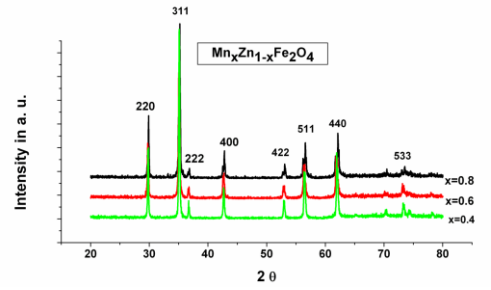

Figure 1. XRD pattern of $Mn_xZn_{1-x}Fe_2O_4$

$$\frac{1}{d_{hkl}} = \frac{\sqrt{h^2+k^2+l^2}}{a} \text{ ---------- Eq.(1)}$$

$$D = \frac{0.9\lambda}{\beta \, Cos\, \theta} \text{ --------- Eq.(2)}$$

The deviation of lattice constant and variation in particle sizes with respect to the concentration abundance of Mn in sample stoichiometry are tabulated in table1. The lattice constant 'a' (8.4748 Å for x=0.4 with consistent gradual increase up to 8.4848 Å for x=0.8) is in good agreement with numerous literature reports [15]. However the particle sizes although well within nano range do not show any specific trend with respect to Mn concentration.

Table.1. Lattice constant & Particle Size of targe material

Mn concentration X	Lattice Constant in Å	Particle Size in nm
0.4	8.474829	36.00
0.6	8.484757	46.00
0.8	8.484883	34.85

All three samples showed characteristic spinnel IR absorption spectra with absorption bands as shown in Fig.2. The two sets of absorption bands one between 375-450 cm^{-1}(v_1) and the other between 550-610 cm^{-1} (v_2) ,which is a common feature for ferrite material in general was observed for all the three samples. It is also observed that the Me_T-Me_O stretching vibration at 350-330cm^{-1} merges with the Me_O-O stretching vibrations at 450-485cm^{-1}. The observed higher band is due to Me_T-O-Me_O stretching vibrations. Me_O is metal in the octahedral site, Me_T metal in tetrahedral site and O represent oxygen. This reveals the formation of single phase spinel structure with two sub lattices [15].

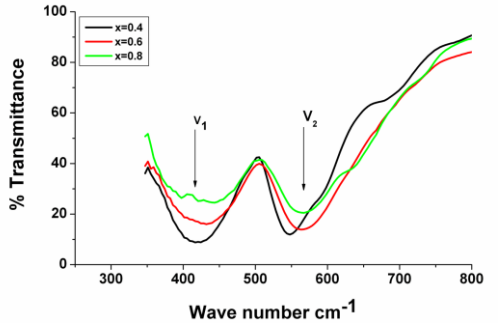

Figure 2. FT- IR absorption spectra of $Mn_xZn_{1-x}Fe_2O_4$

Morphology investigations of the powder samples were carried out using transmission electron microscope and average particle size assessment performed on TEM micrographs. The TEM micrographs were obtained by suspension of particles in isopropane. A typical TEM picture for sample $Mn_{0.8}Zn_{0.2}Fe_2O_4$ is shown in (Fig.3).The micrograph indicate near spherical shape morphology with fair agglomeration. The agglomeration is due to magnetic nature of nanoparticles and may be happening with in the time lag between suspension of particles in isopropane and actual measurement. The individual particles sizes appearing in TEM micrographs were observed to be in concurrence with grain sizes determined from XRD data.

The achieved film thickness on substrate by PLD process is gauged with a stylus prolifreometer by measuring the step height created by an appropriate masking technique during film growth. The measured film thickness along with derived particle size from AFM data is tabulated in table.2

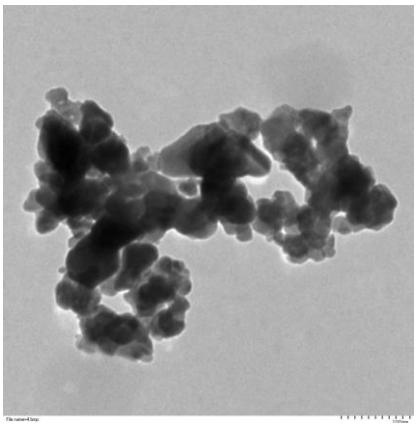

Figure 3.TEM monograph of $Mn_{0.8}Zn_{0.2}Fe_2O_4$

Table.2.Thickness and particle size of $Mn_xZn_{1-x}Fe_2O_4$ thin films.

Mn concentration x	Thickness in Å	Particle Size in nm
0.4	1500	37
0.6	1050	45
0.8	1100	41

The formations of crystalline ferrite thin films were confirmed by x-ray diffraction technique. The XRD pattern of all three deposited thin films are shown in Fig.4

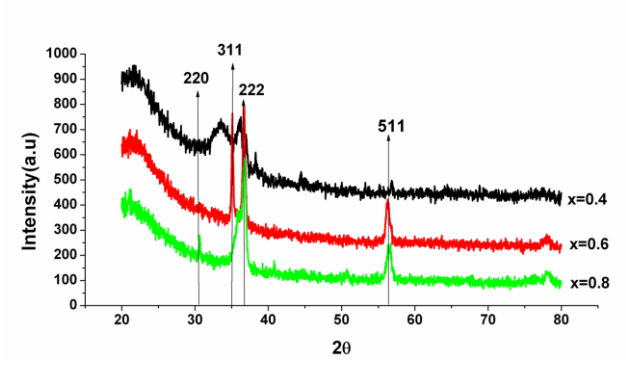

Figure 4. XRD pattern of $Mn_xZn_{1-x}Fe_2O_4$ thin films.

All visible XRD peaks, pertaining to the three thin film samples were indexed to the spinel phase. The observation of non appearance of certain identified ferrite XRD peaks and abnormally high intensity for some observed XRD peaks in comparison to the peak arising out of reflections from (311) crystallographic plane is attributed to crystallographic texture. Further the observation of minimal number of visible peaks in sample with lowest Mn concentration gives a clear indication of preferred crystallographic orientation resulting in strong texture. The degree of texture, which dependents on the percentage of crystals having the preferred orientation, decreases with increase in Mn concentration. A small shift in peak position with respect to the target material, visible in thin film XRD, is indicative of variation in lattice parameter. This difference may be ascribed to local stresses [16,17] arising from atomic peening observed in planer natured materials like thin films. In PLD process the bombardment of the substrate layer by energetic particulate matter in laser plume generates a compressive stress in the planes parallel to the surface which in turn creates an expansion in the planes normal to the surface. This causes an increase in the lattice parameter normal to the surface, which explains the observed shift noticed on the X-ray spinel peaks of the films.

AFM images (Fig.5,6&7) of the thin film samples showed homogeneous morphology surfaces with spherical particles of regular size and uniform distribution.

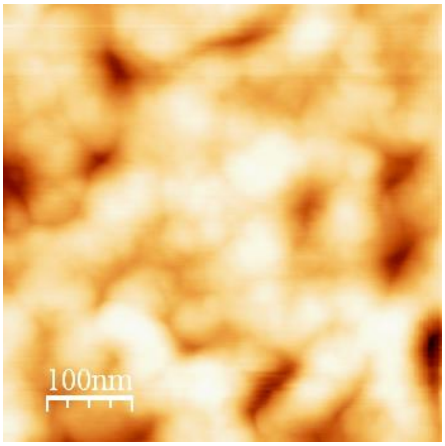

Figure 5. AFM images of $Mn_xZn_{1-x}Fe_2O_4$ thin film (x=0.4).

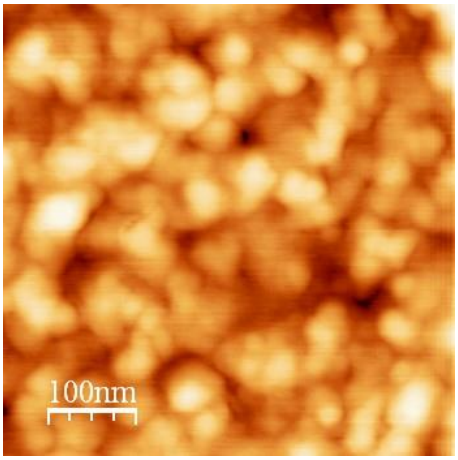

Figure 6. AFM images of $Mn_xZn_{1-x}Fe_2O_4$ thin film (x=0.6).

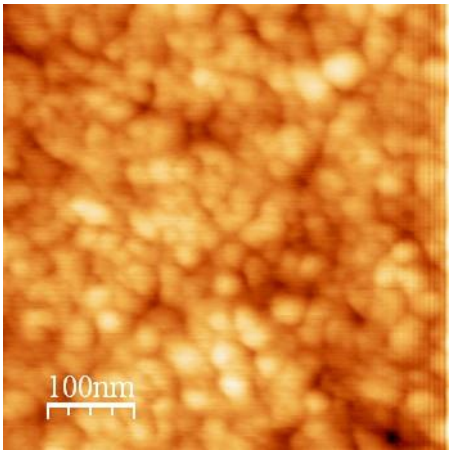

Figure 7. AFM images of $Mn_xZn_{1-x}Fe_2O_4$ thin film (x=0.8).

The films with higher Mn concentration(x=0.8) had a smoother surface. As Mn concentration decreases a ridge like morphology sets in which is predominantly visible in AFM image of sample x=0.4. The derived roughness average from AFM data is plotted in Fig.8

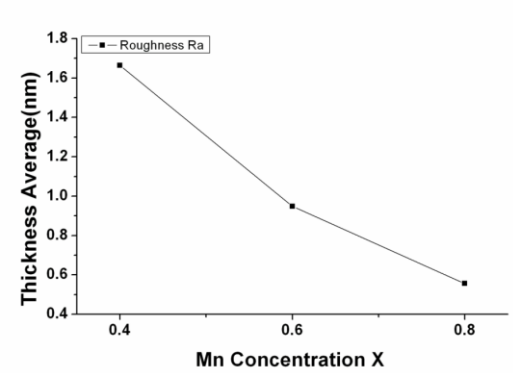

Figure 8. Roughness average of $Mn_xZn_{1-x}Fe_2O_4$ thin films.

The diameters of all predominant particles appearing on film surface viewed through AFM were determined using a particle analysis tool and averaged for estimation of particle size. The average estimated particles sizes of all three samples are tabulated in table.2 which confirms nanogranular morphology with dimensions similar to the target particles. This mach in dimensions is achieved by optimization of deposition temperature, nature of substrate and energy fluence, a critical process parameter.

Magnetic properties of ferrite thin films depend on the magnetic-crystalline anisotropy, the grain size and surface morphology of the films [18-20]. The *M-H* loops of the thin films recorded at room temperature using a SQUID VSM are as shown in Fig. 9.

The substrate contribution to the *M-H* loop was subtracted after obtaining the loops. It can be seen that the deposited material on all films are magnetically ordered at room temperature and saturate at normal values of applied magnetic field.

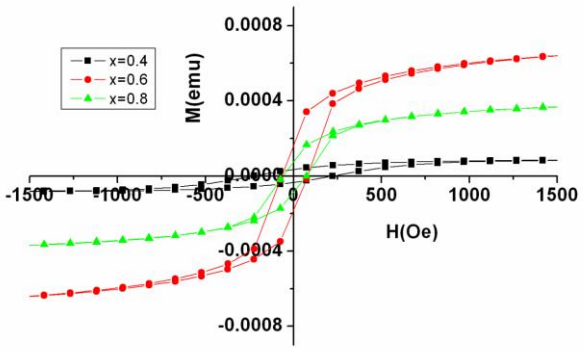

Figure 9. M-H loops of $Mn_xZn_{1-x}Fe_2O_4$ thin films

The hysteresis loss factor that is minimum for concentration x=0.4, increased for x=0.6 and drops noticeably for x=0.8. The X and Y axis intercept values indicative of coercivity and remnant magnetization of thin film samples is tabulated in table.3.

Fig.10 provide a comprehensive visual expression of data for comparison of coercivity, where in thin film with concentration x=0.4 possess relatively high value. A substantial shift in peak position for sample X=0.4 in comparison to the other two samples in XRD data indicate the presence of a relatively large lattice strain for this particular sample. The presence of lattice strain can cause a large magnetic anisotropy and therefore lead to high coercivity [18, 19].

Further an amount of disorder at the surface can also influences the magnetic property coercivity, [18-20]. Therefore the ridge like formation observed in AFM image of the sample X=0.4, which invariably increases the roughness of the surface might have contributed to the observation of high coercivty.

Table.3. Coercivity & Remanant magnetisation of $Mn_xZn_{1-x}Fe_2O_4$ thin films.

Mn concentration x	X-Axis Intercept. (coercivity)	Y-Axis Intercept. (remnant magnetization)
0.4	228.43 -220.04	$3.40x10^{-5}$ $-3.45x10^{-5}$
0.6	74.92 -69.68	$1.70x10^{-4}$ $-1.76x10^{-4}$
0.8	78.58 -75.09	$7.72x10^{-5}$ $-8.55x10^{-5}$

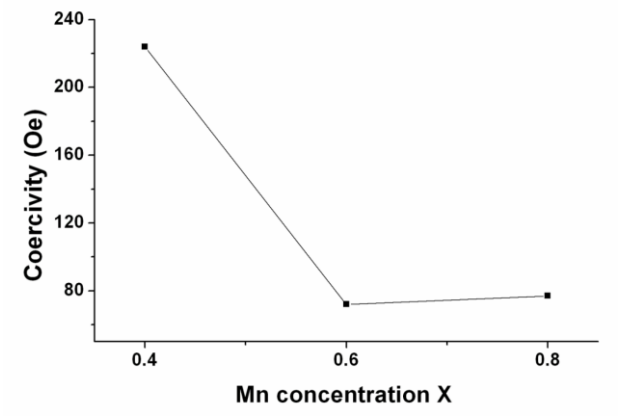

Figure 10. Coercivity of $Mn_xZn_{1-x}Fe_2O_4$ thin films.

The formation of ridge like morphology which is predominant for sample x=0.4 and decreases with increase in Mn concentration as seen from AFM images can be attributed to directional film growth catapulted by initial low number of nucleation sites on target surface. A probable reason for the decrease in number of initial nucleation sites for samples having lower Mn concentration may be the variation in adsorption property of substrate film pair which depends on chemical composition of the sample.

4. Conclusions

Polycrystalline ferrite nanoparticles of $Mn_xZn_{1-x}Fe_2O_4$ (x=0.4,0.6&0.8) were prepared by co-precipitation method. The samples were characterized using XRD and FT-IR techniques. Particle sizes were estimated from XRD data and corroborated with TEM micrographs. Thin films of these samples were fabricated by PLD technique and characterized using XRD. The presence of nano granular morphology in films with dimensions comparable to that of target material grain is confirmed using AFM images. Thin film XRD data indicate film growth with moderate texture, with its degree decreasing with increase in Mn concentration. *M-H* loops of these thin films revealed enhanced coercivity which is explained on the basis of texture enhanced lattice strain and observed surface disorder. An expected reason for surface disorder seems to be directional film growth catapulted by initial low number of nucleation sites on target surface. The reason for decline in number of nucleation sites with respect to sample composition may be the variation in adsorption property of substrate film pair.

Acknowledgements

The first author acknowledges the use of PLD, XRD, AFM, and SQUID VSM from UGC-DAE-CSR Indore.

References

[1] N. Yamazoe, Sens. Actuators, B, Chem. **5**, p. 7. (1991),

[2] Williams C, Chrisey D, Lubitz P, Grabowski K, Cotell C. J Appl Phys **75**,1676. (1994)

[3] W. Gopel and D. Schierbaum, Sens. Actuators, B, Chem. **26** (1–3), p. 1. (1995)

[4] G. Behr and W. Fhegel, Sens. Actuators, B, Chem, **33–37** p. 2627. (1995)

[5] C.H. Kwon, H.-K. Hong, D.H. Yun, K. Lee, S.-T. Kim, Y.-H. Roh and B.-H. Lee, Sens. Actuators, B, Chem. **24–25** p. 610. (1995)

[6] G. Magamma, V. Jayaraman, T. Gnanasekaran and G. Periaswami, Sens. Actuators, B, Chem, **53** p. 133. (1998)

[7] Miyanishi S, Iketani N, Takayama K, Innami K, Suzuki I, Kitazawa T, Ogimoto Y, Murakami Y, Kojima K and Takahashi A IEEE Trans. Magn. **41** 2817(2005)

[8] Williams M C, Chrisey B D, Lubits P, Grabowski S K and Cotell M J. Appl. Phys. **75,** 1676,(1994)

[9] Hae Seok Cho, Hyeong Joon Kim,. Appl. Phys. Lett. **66** (10), 6,March (1995)

[10] Y. Suzuki R. B. van Dover, E. M. Gyorgy,b) Julia M. Phillips, V. Korenivski, D. J. Werder, C. H. Chen, R. J. Cava, J. J. Krajewski, and W. F. Peck, Jr. Appl. Phys. Lett. **68** (5), 29 January (1996)

[11] Masaki Nakano, Jae Man Song, Hirotoshi Fukunaga, and Yoshio Matsuo, IEEE transactions on magnetics, vol. **36**, no. 5, 11 september (2000).

[12] Jeong Sik Lee Tae Wook Haa,, Jung Hyun Jeongb, Ill Won Kimc, Soung Soo Yid Thin Solid Films **472**,217–221,(2005)

[13] Yan Liu Jiangwei Cao, Zheng Yang Materials Science and Engineering B **127** 108–111,(2006)

[14] Hideki Etoh1,2 Junichi Sato2, Yoshiteru Murakami2, Akira Takahashi2 and Ryoichi Nakatani1 Journal of Physics: Conference Series **165**, 012031(2009)

[15] Tangsali R B, Keluskar S H, Naik G K, Budkuley J S, Int. J. Nanoscience, Volume: **3**, Issues: 4-5 pp.589-597. (2004),

[16] A. Lisfi and C. M. Williams, J. Appl. Phys. **93**, 8143 (2003)

[17] A. Lisfi, J. C. Lodder, E. G. Keim, and C. M. Williams, Appl. Phys. Lett. **82**, 76 (2003)

[18] Ultrathin Magnetic Structures I and II,ed.by J. A.C.Bland and B.Heinrich (Springer, NewYork, 1994)

[19] Y.-P. Zhao, R.M. Gamache, G.-C. Wang, T.-M. Lu, G. Palasantzas, J.Th.M. De Hosson, J. Appl. Phys. **89**, 13 25 (2001)

[20] Y. P. Zhao, G. Palasantzas, G. -C. Wang, T. -M.Lu, and J. Th. M. De Hosson, Phys. Rev. B **60**, 1216 (1999).